Scattering of GeV electrons by light nuclei

O. Benhar* and V. R. Pandharipande
Department of Physics, University of Illinois, 1110 West Green Street, Urbana, Illinois 61801
(Received 12 November 1992)

The cross section for inclusive scattering of high-energy electrons by ^{2}H, ^{3}He, and ^{4}He with momentum transfer $|\mathbf{q}| \sim 2$ GeV/c is calculated using realistic spectral functions. The final-state interaction effects are treated with the correlated Glauber approximation, and the possible occurrence of color transparency is considered. The results are in fair agreement with the SLAC data and confirm the presence of high-momentum components in the deuteron wave function. The final-state interaction effects are significant in ^{3}He and ^{4}He, and there seem to be systematic differences between theory and experiment at large ω in ^{4}He.

PACS number(s): 21.45.+v, 25.30.Fj

I. INTRODUCTION

During the past decade, inclusive electron-nucleus scattering experiments have provided important information on both the structure and the electromagnetic interactions of nuclei (for recent reviews see Ref. [1]). Of particular relevance are the measurements carried out using multi-GeV electrons, since the high momentum transfers attainable give access to the short interparticle distance behavior of the nuclear wave function, whose knowledge may provide a deeper understanding of nuclei. The pioneering (e,e') experiments in this kinematical regime have been performed using ^{2}H [2] and ^{3}He [3] targets. More recently, a systematic experimental study has been carried out for a variety of heavier systems, ranging from ^{4}He to ^{197}Au [4], and from the analysis of the mass dependence of the data, the inclusive cross section for infinite nuclear matter has been extracted [5]. The few nucleon systems ($A \leq 4$) and infinite nuclear matter are best suited for a significant comparison between theoretical predictions and experimental data, since accurate calculations are feasible.

The behavior of the (e,e') cross section at fixed momentum transfer $\mathbf{q}$, as a function of the electron energy loss ω, is characterized by a wide peak centered at $\omega \sim \sqrt{\mathbf{q}^2+m^2}-m$, m being the nucleon mass, produced by quasielastic single nucleon processes. As the momentum transfer $\mathbf{q}$ increases, however, the quasielastic peak is obscured by the contributions coming from inelastic processes, such as excitation of nucleon resonances and deep inelastic scattering, leading to complex hadronic final states. These gross features are fairly well reproduced by the theoretical calculations carried out for ^{3}He [6] and infinite nuclear matter [7] using the plane-wave impulse approximation (PWIA) and nuclear spectral functions obtained from microscopic calculations. However, a sizable disagreement between PWIA predictions and experiments occurs in the low-energy loss region, where the calculated cross sections consistently underestimate the data.

The quantitative understanding of the low ω tail of the inclusive cross section, where the inelastic contributions are negligible, is particularly relevant. According to the PWIA picture, the dominant reaction mechanism in this region is the scattering of the electron by a strongly correlated nucleon of high initial momentum. This feature was pointed out in the 1960s by Czyz and Gottfried [8], who argued that the (e,e') cross section at high momentum transfer and low energy loss measures the high-momentum components of the target wave function, thus providing important information on short-range nucleon-nucleon (NN) correlations. The analysis of the available data in terms of the scaling variable y [4,9,10], however, clearly shows that in the low-energy loss region, corresponding to $y \ll 0$, significant scaling violations occur, indicating the breakdown of PWIA due to the final-state interactions (FSI) between the struck nucleon and the residual nucleus. It appears that momentum transfers < 3 GeV/c are not high enough, and the kinematical regime in which the (e,e') cross section can simply be expressed in terms of the elementary electron-nucleon cross section and the nuclear spectral function $P(\mathbf{k},E)$, giving the probability of removing a nucleon of momentum $\mathbf{k}$ from the target by transferring energy E to the residual system, has not been reached.

In Ref. [7] the effect of the FSI on the inclusive cross section for nuclear matter (NM) has been evaluated with a generalization of the Glauber theory [11] suitable to describe the motion of the struck nucleon through the nuclear medium. The modification of the FSI coming from the possible occurrence of the phenomenon generally referred to as color transparency [12,13] has also been investigated. The FSI redistribute the strength predicted by PWIA; the quasifree peak is slightly reduced and the low ω tail of the cross section is greatly enhanced. The theoretical results of Ref. [7] are in good agreement with the data over a range of momentum transfer 1.5 GeV/$c \lesssim q \lesssim 2.5$ GeV/c.

In this paper the approach developed in Ref. [7] is extended to the study of the inclusive cross section of ^{2}H, ^{3}He, and ^{4}He at momentum transfer $q \sim 2$ GeV/c. For

*On leave from INFN, Sezione Sanita, I-00161 Rome, Italy.

the two- and three-body systems we have employed the full spectral functions obtained from microscopic calculations, whereas the $P(\mathbf{k},E)$ for ^{4}He has been approximated assuming that the one- and two-body terms give the dominant contributions. In Sec. II we briefly recall the structure of the (e,e') cross section within PWIA, whereas in Sec. III the spectral functions employed in the calculations are described. Section IV is devoted to the discussion of the correlated Glauber approximation (CGA) used to include FSI effects and in Sec. V the theoretical results are discussed and compared with the data.

II. THE (e,e') CROSS SECTION WITHIN PWIA

The differential cross section for the process $e+A\rightarrow e'+anything$, in which an electron of initial four-momentum $k\equiv(\varepsilon,\mathbf{k})$ scatters off a nuclear target to a state of four-momentum $k'\equiv(\varepsilon',\mathbf{k}')$, the target final state being undetected, can be written in Born approximation as [14]

$$\frac{d^2\sigma}{d\Omega\, d\varepsilon'}=\frac{\alpha^2}{Q^4}\frac{\varepsilon'}{\varepsilon}L^{\mu\nu}W^A_{\mu\nu}\ , \tag{2.1}$$

where $Q=k-k'\equiv(\omega,\mathbf{q})$ is the four-momentum transfer and α is the fine structure constant. The leptonic tensor $L^{\mu\nu}$ is completely determined by the electron momenta $\mathbf{k}$ and $\mathbf{k}'$, whereas all the information on the target structure is embedded in the nuclear tensor $W^A_{\mu\nu}$, whose definition involves the initial and final nuclear states $|0\rangle$ and $|N\rangle$, with four-momenta p_0 and p_N, as well as the nuclear current operator J^A_μ:

$$W^A_{\mu\nu}(\mathbf{q},\omega)=\sum_N \langle 0|J^A_\mu|N\rangle\langle N|J^A_\nu|0\rangle\delta^{(4)}(p_0+Q-p_N)\ . \tag{2.2}$$

Calculations of $W^A_{\mu\nu}$ for moderate momentum transfers ($q\lesssim 0.5$ GeV/c) can be carried out within the nuclear many-body theory (NMBT) using nonrelativistic wave functions to describe the nuclear initial and final states, and expanding the current operator in powers of (q/m) (see, e.g., Refs. [15,16]). At the higher values of q corresponding to multi-GeV incident electrons, however, the description of the final states $|N\rangle$ in terms of nonrelativistic nucleons is no longer possible, and some simplifying assumptions have to be made in order to take into account the relativistic motion of the struck particle and the occurrence of inelastic electron-nucleon scattering processes, leading to the appearance of excited hadronic states, mesons, etc.

A reasonable approximation scheme to describe the high momentum transfer region is based on the following assumptions. First is that the nuclear current operator J^A_μ can be approximated by a sum of one-nucleon currents, and the second is that the spectral function of the target can be estimated with the nonrelativistic NMBT, so that only the motion of the struck nucleon has to be treated relativistically. The simplest possible implementation of this picture of electron-nucleus scattering is provided by the PWIA, in which the struck nucleon propagates freely through the residual $(A-1)$-nucleon state. The resulting expression for the nuclear tensor is

$$W^A_{\mu\nu,\mathrm{IA}}(\mathbf{q},\omega)=\int d\mathbf{k}\, dE[ZP^p(\mathbf{k},E)\tilde{W}^p_{\mu\nu}(\mathbf{q},\omega,\mathbf{k},E)+(A-Z)P^n(\mathbf{k},E)\tilde{W}^n_{\mu\nu}(\mathbf{q},\omega,\mathbf{k},E)]\ , \tag{2.3}$$

where $P^{p\,(n)}(\mathbf{k},E)$ denotes the proton (neutron) spectral function and $\tilde{W}^{p\,(n)}_{\mu\nu}$ is the electromagnetic tensor of a bound proton (neutron).

The difference between $\tilde{W}_{\mu\nu}$ and the corresponding quantity for a free nucleon, $W_{\mu\nu}$, comes from the fact that, when the electron scatters off a bound nucleon of momentum $\mathbf{k}$, part of the energy loss ω goes into the spectator system. In Ref. [17] de Forest proposed to write $\tilde{W}_{\mu\nu}$, for quasielastic scattering using the free nucleon spinors and current operators. This leads to the following definition of the energy transfer to the struck nucleon, $\tilde{\omega}$:

$$\tilde{\omega}=\sqrt{(\mathbf{k}+\mathbf{q})^2+m^2}-\sqrt{k^2+m^2}=\omega-E-(\sqrt{k^2+m^2}-m)\ . \tag{2.4}$$

The requirement of gauge invariance,

$$Q_\mu\tilde{W}^{\mu\nu}=\tilde{W}_{\mu\nu}Q^\nu=0\ , \tag{2.5}$$

is also fulfilled within the prescription of Ref. [17]. The time components of $\tilde{W}_{\mu\nu}$ are assumed to be the same as those of $W_{\mu\nu}(\mathbf{q},\tilde{\omega})$ and the longitudinal components are expressed in terms of the time components according to Eq. (2.5). Taking the z axis along the direction of $\mathbf{q}$, the following relations are obtained:

$$\begin{aligned}&\tilde{W}_{\mu\nu}(\mathbf{q},\omega,\mathbf{k},E)=W_{\mu\nu}(\mathbf{q},\tilde{\omega}),\quad \text{for } \mu \text{ and/or } \nu=0\ ,\\ &\tilde{W}_{3\mu}(\mathbf{q},\omega,\mathbf{k},E)=\left[\frac{\omega}{q}\right]W_{0\mu}(\mathbf{q},\tilde{\omega})\ .\end{aligned} \tag{2.6}$$

This procedure, which has been followed in Ref. [7] and in the present work, is manifestly not unique. However, it has been shown that, at high momentum transfer, the PWIA cross section for ^{3}He obtained with a different off-shell extrapolation, in which Eq. (2.5) is used to eliminate the dependence upon the time components of $\tilde{W}_{\mu\nu}$, are very close to those evaluated according to the de Forest prescription [6].

III. THE SPECTRAL FUNCTIONS OF THE FEW-NUCLEON SYSTEMS

The spectral function, i.e., the probability distribution of removing a particle of momentum $\mathbf{k}$ from the nuclear ground state leaving the residual system with an energy E_0+E, can be written as

$$P(\mathbf{k},E)=\sum_n |\langle n|a_k|0\rangle|^2\delta(E+E_0-E_n)\ , \tag{3.1}$$

where $|0\rangle$ is the nuclear ground state, with energy E_0, whereas $|n\rangle$ and E_n are the eigenstates and energies of the $(A-1)$-nucleon system, respectively. The state $|n\rangle$ has momentum $-\mathbf{k}$, and its energy E_n include the recoil

kinetic energy $k^2/2M_R$, where M_R is the mass of $|n\rangle$. In literature $P(\mathbf{k},E)$ has also been defined with $\delta(E+E_0-(E_n-k^2/2M_R))$ in place of the δ function in Eq. (3.1).

It clearly appears from Eq. (3.1) that the spectral function of the deuteron can be readily expressed in terms of the momentum distribution $n_d(k)$ of nucleons in the deuteron:

$$P(\mathbf{k},E)=n_d(k)\delta(E+E_d-k^2/2m)\ , \tag{3.2}$$

E_d being the deuteron energy. The present calculations for ^{2}H have been carried out using the momentum distribution calculated with the Argonne NN interaction [18]. In order to study the magnitude of the effect of relativistic correction to the energy of the recoiling nucleon, we have also used the spectral function:

$$P_{RR}(k,E)=n_d(k)\delta(E+E_d-\sqrt{k^2+m^2}+m) \tag{3.3}$$

for the deuteron. The $P(k,E)$ and $P_{RR}(k,E)$ give rather similar results as discussed in Sec. V.

In the case of the three-nucleon system one has to include in Eq. (3.1) the states $|n\rangle$ corresponding to the deuteron with momentum $-\mathbf{k}$ and continuum two-nucleon states with momentum $-\mathbf{k}$. In PWIA these states, respectively, give the two- and three-body breakup channels. Microscopic calculations of $P(\mathbf{k},E)$ have been carried out within a variational approach, in which the three-nucleon bound state wave function is expanded in a series of harmonic-oscillator states [19], as well as using the solution of the Faddeev equation in momentum space [20]. The results discussed in Sec. V have been obtained using the spectral function of Ref. [20], corresponding to the Paris NN interaction [21], as well as with an approximate $P(\mathbf{k},E)$ described below.

The $P(\mathbf{k},E)$ of ^{4}He has been studied by Morita and Suzuki [22] by the ATMS (amalgamation of the two-body correlation into the multiple scattering process) method. In the present work we have used an approximate method of the type discussed in Ref. [23]. This method uses the available results of the momentum distribution of the nucleons $[n(k)]$, ^{3}He$+n$ and ^{3}H$+p$ states $[n_{3,1}(k)]$ and that of the d-d state $[n_{dd}(k)]$ in ^{4}He. The contribution $P_1(\mathbf{k},E)$ of the states $|n\rangle$ corresponding to ^{3}H or ^{3}He with momentum $-\mathbf{k}$ is directly given by $n_{3,1}(k)$:

$$P_1(\mathbf{k},E)=n_{3,1}(k)\delta(E+E_4-E_3-k^2/2m_3)\ , \tag{3.4}$$

where E_4 is the energy of ^{4}He and E_3 is the energy of ^{3}H (^{3}He) for proton (neutron) $P_1(\mathbf{k},E)$. The remaining $P_R(\mathbf{k},E)$ is defined as

$$P_R(\mathbf{k},E)=P(\mathbf{k},E)-P_1(\mathbf{k},E) \tag{3.5}$$

and

$$\int P_R(\mathbf{k},E)dE=n(k)-n_{3,1}(k)\ . \tag{3.6}$$

The $P_R(\mathbf{k},E)$ provides $\sim$20% of the normalization of $P(\mathbf{k},E)$, coming mostly from large values of k. It represents the contribution from the a_k in $P(\mathbf{k},E)$ of Eq. (3.1) annihilating one of a correlated pair of nucleons. If we neglect the total momentum of the correlated pair, then the resulting three-body final state has a nucleon with momentum $-k$ and a leftover pair of nucleons with zero total momentum. In this approximation

$$P_R(k,E)=[n(k)-n_{3,1}(k)]\delta(E+E_4-k^2/2m)\ , \tag{3.7}$$

assuming that the leftover pair has negligible energy.

The correlations are strongest in the $T=0$ $S=1$ deuteronlike states. Hence it is probably more accurate to approximate the momentum distribution of the correlated pairs by that of deuterons in ^{4}He, than to neglect it completely. In this case we obtain

$$P_R(\mathbf{k},E)\sim c(k)\int d\mathbf{k}_p n_d(|\mathbf{k}-\tfrac{1}{2}\mathbf{k}_p|)n_{dd}(k_p)\delta \times\left[E+E_4-E_d-\frac{k_p^2}{2m_d}-\frac{(\mathbf{k}-\mathbf{k}_p)^2}{2m}\right]\ , \tag{3.8}$$

and the constant $c(k)$ is determined from Eq. (3.6).

In the present work we have employed the approximations (3.7) and (3.8) to estimate the ^{4}He spectral function using the deuteron momentum distribution of Ref. [18] and $n(k)$, $n_{3,1}(k)$, and $n_{dd}(k)$ resulting from the Monte Carlo calculations of Ref. [24], with the Argonne $v_{14}+$Urbana VIII interactions.

A test of the validity of the approximations implied in the calculation of $P(\mathbf{k},E)$ of ^{4}He has been made using the procedure described in Eqs. (3.5) and (3.8) to evaluate the ^{3}He spectral function from the $n(k)$ and $n_{2,1}(k)$ [24] in ^{3}He. The quasielastic PWIA cross sections obtained with the approximate $P(\mathbf{k},E)$ are very close to those with the spectral function of Ref. [20] as can be seen in Fig. 1 for the case of incident electron energy $\varepsilon=10.954$ GeV and scattering angle $\theta=8°$.

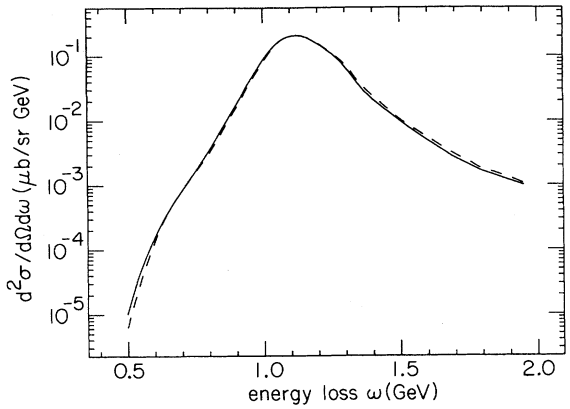

FIG. 1. The PWIA cross section for quasielastic scattering of 0.954 GeV electrons by 8° off ^{3}He. The full and dashed curves re obtained with the Hannover [20] and the approximate spec-al functions.

IV. THE CORRELATED GLAUBER APPROXIMATION FOR FINAL-STATE INTERACTION

The approximation scheme called CGA, employed to improve upon PWIA for nuclear matter [7], can be better

understood by rewriting the nuclear tensor of Eq. (2) in the form

$$W^A_{\mu\nu}(\mathbf{q},\omega)=\int \frac{dt}{2\pi} e^{i(\omega+E_0)t}\langle 0|J^A_\mu e^{-iHt} J^A_\nu|0\rangle \ , \tag{4.1}$$

and taking into account quasielastic electron-nucleon processes only. In the kinematical regime discussed in the present paper, the inelastic contributions are very small in the low-energy loss region, where FSI effects are important, and hence it is reasonable to treat them with PWIA.

Replacing the nuclear current J^A_μ with the sum of the one-body nucleon currents j^l_μ and keeping only the terms corresponding to incoherent scattering processes, which are known to be dominant at high momentum transfer, the matrix elements of Eq. (4.1) can be rewritten in the coordinate representation as

$$W^A_{\mu\nu}(\mathbf{q},\omega)=\sum_{l=1}^{A}\int \frac{dt}{2\pi} e^{i(\omega+E_0)t}\int dR\, dR' e^{-i\mathbf{q}\cdot(\mathbf{r}_l-\mathbf{r}_l')}\Psi_0^*(R) j^l_\mu U(R,R';t) j^l_\nu \Psi_0(R') \ , \tag{4.2}$$

where $R\equiv\{\mathbf{r}_1,\ldots,\mathbf{r}_A\}$ denotes the set of coordinates specifying the configuration of the target and Ψ_0 is the ground-state wave function. The price paid for eliminating the sum over the final states from the definition of the nuclear tensor is the introduction of the propagator

$$U(R,R';t)=\langle R|e^{-iHt}|R'\rangle \ , \tag{4.3}$$

describing the evolution of the interacting A-particle system from the configuration R' to the configuration R during the time interval t.

The PWIA form of the nuclear tensor, given by Eq. (2.3), can be obtained from Eq. (4.2) by considering

$$H=H_{A-1}+H_0 \ , \tag{4.4}$$

where H_{A-1} and H_0 are the Hamiltonians of the interacting spectator system and of a free nucleon, respectively. With the Hamiltonian (4.4) the propagator reduces to the factorized form

$$U_{\mathrm{PWIA}}(R,R';t)=U_{A-1}(\tilde{R},\tilde{R}';t)U_0(\mathbf{r}_1;\mathbf{r}_1';t) \ , \tag{4.5}$$

where we have taken $l=1$ for convenience, and $\tilde{R}\equiv\{\mathbf{r}_2,\ldots,\mathbf{r}_A\}$. Using the spectral representations,

$$U_{A-1}(\tilde{R},\tilde{R}';t)=\sum_n \Phi_n(\tilde{R})\Phi_n^*(\tilde{R}')e^{-iE_n t} \ , \tag{4.6}$$

where Φ_n are the eigenstates of the $(A-1)$-particle system with energies E_n, and

$$U_0(\mathbf{r}_1,\mathbf{r}_1';t)=\int d\mathbf{p}\, e^{-iE_p t} e^{i\mathbf{p}\cdot(\mathbf{r}_1-\mathbf{r}_1')} \ , \tag{4.7}$$

where $E_p=\sqrt{p^2+m^2}-m$, Eq. (2.3) can be recovered.

The simplest possible improvement upon PWIA implies the inclusion in Eq. (4.4) of a one-body potential V describing the interaction of the struck particle with the spectator system. This improvement obviously preserves the factorization property of the A-particle propagator, however, the U_0 in Eq. (4.7) must be replaced by

$$U_1(\mathbf{r}_1,\mathbf{r}_1';t)=\langle \mathbf{r}_1|e^{-i(H_0+V)t}|\mathbf{r}_1'\rangle \ . \tag{4.8}$$

The evaluation of this U_1 in general involves a path integration in the space of the functions $\mathbf{r}(\tau)$ satisfying the boundary conditions $\mathbf{r}(0)=\mathbf{r}_1'$ and $\mathbf{r}(t)=\mathbf{r}_1$. For large momentum transfer, however, one can make the hypothesis, as in the standard Glauber theory of scattering [11], that the struck nucleon moves along a straight line with constant velocity $\mathbf{v}$, so that $\mathbf{r}(\tau)=\mathbf{r}_1'+\mathbf{v}\tau$. As a result, U_1 takes the simple eikonal form

$$U_1(\mathbf{r}_1,\mathbf{r}_1';t)=U_0(\mathbf{r}_1,\mathbf{r}_1';t)U_v(\mathbf{r}_1,\mathbf{r}_1';t) \ , \tag{4.9}$$

with

$$U_v(\mathbf{r}_1,\mathbf{r}_1';t)=\exp\left[-i\int_0^t d\tau\, V(\mathbf{r}_1'+\mathbf{v}\tau)\right] \ . \tag{4.10}$$

The complex single-particle optical potential $V(\mathbf{r}_1)$ can be expressed as a sum of two-body interactions between the struck particle with momentum $\sim\mathbf{q}$ and the $(A-1)$ particles in the spectator system:

$$V(\mathbf{r}_1)=\sum_{i=2,A} w(\mathbf{r}_1-\mathbf{r}_i) \ . \tag{4.11}$$

At the high energies of interest we hope that the NN interaction w can be directly related to the NN scattering amplitude $f_q(\mathbf{k})$ at laboratory momentum q and momentum transfer $\mathbf{k}$:

$$w(\mathbf{r})=-\frac{2\pi|\mathbf{v}|}{q}\int \frac{d^3k}{(2\pi)^3} f_q(\mathbf{k})e^{i\mathbf{k}\cdot\mathbf{r}} \ , \tag{4.12}$$

where $q/|\mathbf{v}|=\sqrt{m^2+q^2}$. The imaginary part of $w(r)$ is dominant at large q; it is obtained from the available [25] two-parameter fits:

$$\mathcal{I}f_q(k)=\frac{q}{4\pi}\sigma_{NN}(q)e^{-\beta(q)k^2} \tag{4.13}$$

to the experimental data, and shown in Fig. 2 for two values of q. The real part of $w(r)$ has little effect on the inclusive scattering at large q, as discussed in Ref. [7], and it is neglected here.

In a finite nucleus the $V(\mathbf{r}_1'+\mathbf{v}\tau)$ depends both on the initial position $\mathbf{r}_1'$ of the struck nucleon and the time τ. However, the spectral functions $P(\mathbf{k},E)$ are obtained after spatial integrations, and hence cannot be easily used with the propagator [(4.9) and (4.10)]. Therefore, we further approximate $U_v(\mathbf{r}_1',\mathbf{r}_1,t)$ by averaging over $\mathbf{r}_1'$ in the $V(\mathbf{r}_1'+\mathbf{v}\tau)$. This gives

$$V(\tau)=\int dR|\Psi_0(R)|^2\left[\sum_{i=2,A} w(\mathbf{r}_1+\mathbf{v}\tau-\mathbf{r}_i)\right] \ , \tag{4.14}$$

$$a(t)=\exp\left[\int_0^t \mathcal{I}V(\tau)d\tau\right] \ , \tag{4.15}$$

$$U_1(\mathbf{r}_1,\mathbf{r}_1',t)=U_0(\mathbf{r}_1,\mathbf{r}_1',t)a(t) \ . \tag{4.16}$$

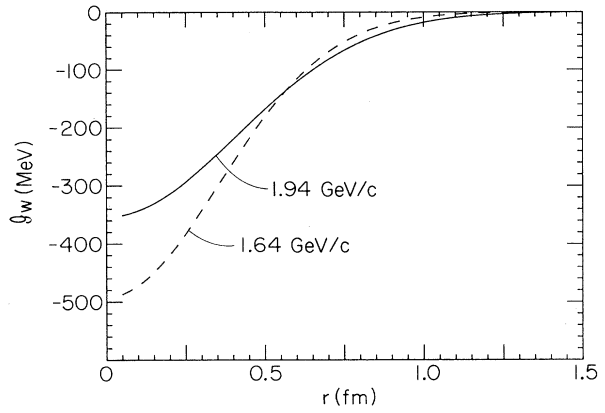

FIG. 2. The imaginary part of $w(r)$ obtained from the two parameter fits to the NN scattering data at lab momenta of 1.94 and 1.64 GeV/c.

The nuclear tensor obtained with the above U_1 is given by the convolution of the PWIA tensor with a folding function:

$$W^A_{\mu\nu}(\mathbf{q},\omega)=\int d\omega' W^A_{\mu\nu,IA}(\mathbf{q},\omega')F_q(\omega-\omega') , \quad (4.17)$$

$$F_q(\omega)=\mathrm{Re}\int_0^\infty \frac{dt}{\pi} e^{i\omega t}a(t) . \quad (4.18)$$

The $V(\tau)$ [Eq. (4.14)] for the deuteron can be easily evaluated from the deuteron wave function, while that for ^{3}He and ^{4}He is obtained with the Monte Carlo method, from configurations distributed with probability $|\Psi_0(R)|^2$. Configurations used in Ref. [24] to study momentum distributions of nucleons, deuterons, and ^{3}H in ^{3}He and ^{4}He, with the Argonne model of v_{NN} and Urbana Model VIII of V_{NNN} were used to calculate $V(\tau)$. The $V(\tau)$ in NM has been calculated in Ref. [7] from the pair distribution functions.

The $a(t)$ calculated for ^{2}H, ^{3}He, ^{4}He, and NM at $|\mathbf{q}|=1.9$ GeV/c are given in Fig. 3. In the finite nuclei $a(t\to\infty)$ approaches a finite value, while in NM $a(t\to\infty)=0$. Thus the $F_q(\omega)$ of finite nuclei contain a δ function of strength $a(t\to\infty)$. The $[a(t\to\infty)]^2$ gives the transparency, i.e., the fraction of struck nucleons that leaves the nucleus without FSI. The $F_q(\omega)$ are shown in Figs. 4(a) and 4(b); those for ^{2}H, ^{3}He, and ^{4}He have the above-mentioned δ function in addition to the $F_q(\omega\pm 0)$.

The validity of the eikonal approximation for the calculation of the one-body propagator has been tested in Ref. [26], where the full inclusive cross section for ^{4}He has been obtained, within a simplified nonrelativistic model, using the path integral Monte Carlo method, and compared to the results using eikonal approximation. It appears from this comparison that the eikonal approximation is sufficiently accurate at $|\mathbf{q}|>1$ GeV/c.

The PWIA cross section is below the data at small ω, in NM [7] as well as in light nuclei, while the cross section obtained by folding PWIA results with $F_q(\omega-\omega')$ [Eq. (4.19)] calculated with the CGA is above the data. Thus, it appears that the CGA $F_q(\omega-\omega')$ overestimates the FSI effects. In Ref. [7] it is shown that the NM results agree with the data when the NN cross section [$\sigma_{NN}(q)$ in Eq. (4.13)] used for calculating the $F_q(\omega-\omega')$

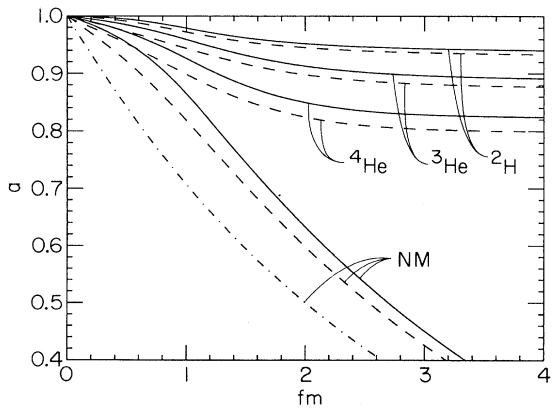

FIG. 3. The decay function $a(t)$ in ^{2}H, ^{3}He, ^{4}He and NM for $|\mathbf{q}|=1.94$ GeV/c. The dashed lines show results obtained with observed $w(r)$ for free nucleons, while the full lines include the effect of the quenching of FSI due to CT. The dash-dotted line shows the $a(t)$ obtained from the free space $w(r)$ in NM without any correlations between nucleons.

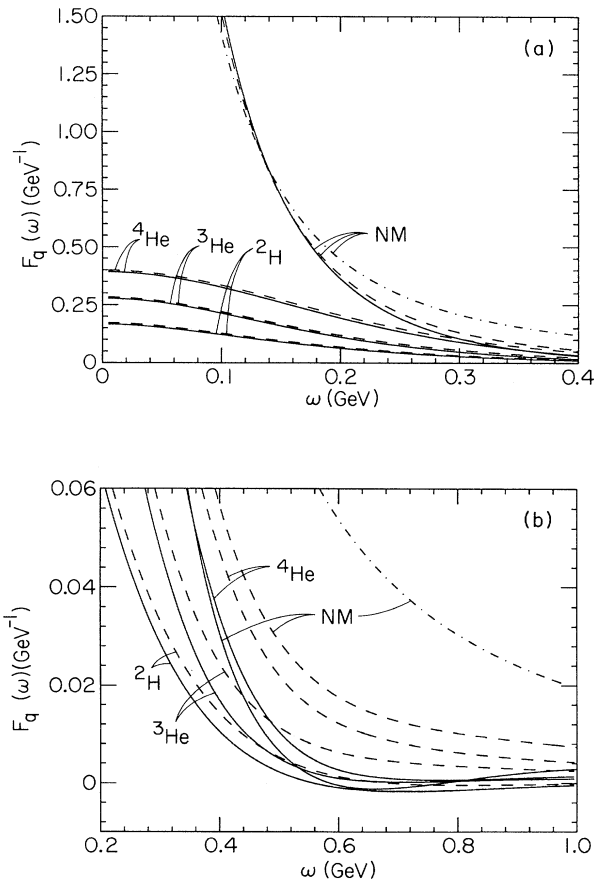

FIG. 4. (a) The folding function $F_q(\omega)$ in ^{2}H, ^{3}He, ^{4}He, and NM for $|\omega|<0.4$ GeV. See the caption of Fig. 3 for notation. (b) the folding function $F_q(\omega)$ in ^{2}H, ^{3}He, ^{4}He, and NM for $|\omega|>0.2$ GeV. See the caption of Fig. 3 for notation.

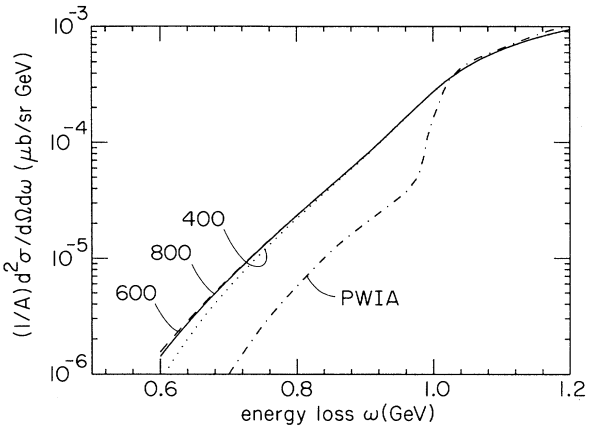

FIG. 5. The PWIA cross section for quasielastic scattering of 3.595-GeV electrons by 30° from NM is shown along with the folded cross sections including FSI effects for $|\omega-\omega'|_{\max}=400$, 600, and 800 MeV.

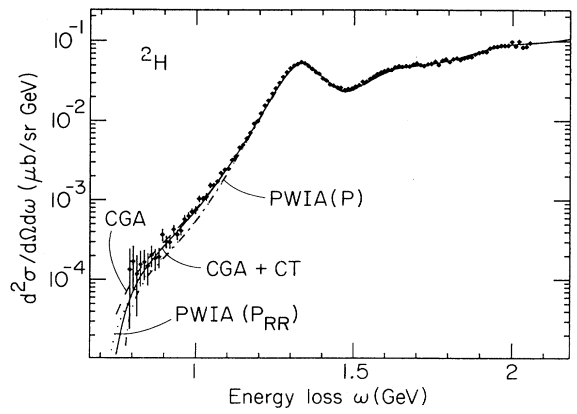

FIG. 6. The experimental and theoretical cross sections for the scattering of 9.76-GeV electrons by 10° from ^{2}H. The dash-dotted, dashed, and full curves, respectively, show results obtained with PWIA, CGA without and with CT effects. The dotted curve shows PWIA results obtained with the $P_{RR}(k,E)$.

is corrected for color transparency (CT) effects [12,13,27]. These effects make the cross section for the scattering of the struck hadron by the other $(A-1)$ nucleons depend upon the distance z traveled by the struck hadron. Following Ref. [27] we use

$$\sigma(z)=\sigma_{NN}S(z)\ , \tag{4.19}$$

$$S(z<l_h)=\left[\frac{z}{l_h}\left[1-\frac{9\langle k_T^2\rangle}{Q^2}\right]+\frac{9\langle k_T^2\rangle}{Q^2}\right]\ , \tag{4.20}$$

$$S(z>l_h)=1\ , \tag{4.21}$$

$$l_h=2E_q/\Delta M^2\ , \tag{4.22}$$

with $\Delta M^2=0.7$ GeV^2 and $\langle k_T^2\rangle^{1/2}=350$ MeV. The effect can be easily included in the CGA by multiplying the $V(\tau)$ [Eq. (4.14)] by $S(|\mathbf{v}|\tau)$. The amplitude $a(t)$ and the folding function $F_q(\omega)$ obtained after including the CT effect are shown in Figs. 3 and 4 by full lines. In these figures we also show the $a(t)$ and $F_q(\omega)$ obtained in NM after ignoring all correlations in the ground state by dash-dotted lines. It should be noted that the suppression of FSI effects by correlation (i.e., the difference between dash-dotted and dashed curves) is larger than that by CT.

The integral in Eq. (4.17) has contributions from the region $|\omega-\omega'|<0.6$ GeV in NM as illustrated in Fig. 5. The cross sections shown in this figure are obtained by $F_q(\omega-\omega')$ which are artificially set to zero for $|\omega-\omega'|>\omega_{\max}$ and labeled with $\omega_{\max}$.

V. RESULTS

The calculated (e,e') cross sections for ^{2}H, ^{3}He, and ^{4}He are compared with the data in Figs. 6–8. The kinematical conditions correspond to incident electron energies and scattering angles: $\varepsilon=9.76$ GeV, $\theta=10°$ for ^{2}H [2], $\varepsilon=10.954$ GeV, $\theta=8°$ for ^{3}He [3], and $\varepsilon=3.595$, $\theta=30°$ for ^{4}He [4]. The momentum transfers are in the $1.8\lesssim|\mathbf{q}|\lesssim2.1$ GeV/c range. The results obtained for

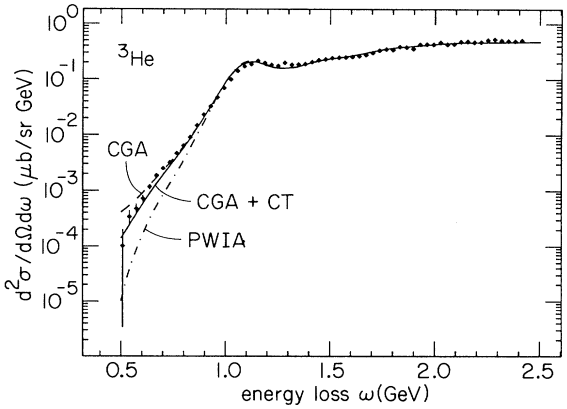

FIG. 7. The experimental and theoretical cross sections for the scattering of 10.954-GeV electrons by 8° from ^{3}He. The dash-dotted, dashed, and full curves, respectively, show results obtained with PWIA, CGA without and with CT effects.

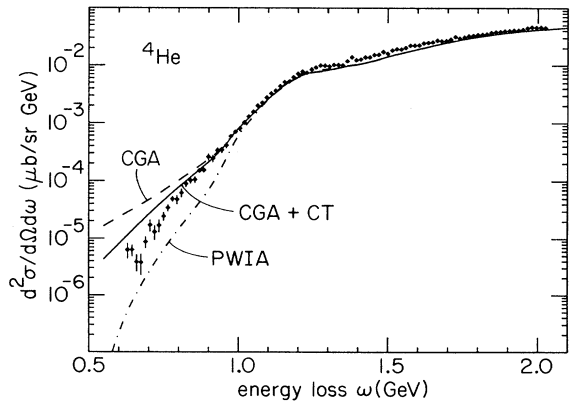

FIG. 8. The experimental and theoretical cross sections for the scattering of 3.595-GeV electrons by 30° from ^{4}He. See the caption of Fig. 7 for notation.

NM in Ref. [7] for $\varepsilon=3.595$ and $\theta=30°$ are shown along with the extrapolated data [5] in Fig. 9 for comparison. The quasielastic contribution to the PWIA cross section is calculated using the parametrization of Ref. [28] for the nucleon form factors. The contribution of the electron-nucleon inelastic processes is obtained from nucleon structure functions extracted from available electron-proton and electron-deuteron scattering data in the resonance and deep inelastic regions [29].

The theory is in very good agreement with the data for ^{2}H and ^{3}He. The PWIA results shown by dash-dotted curves are below the data, while the CGA results without CT effects, shown by dashed lines, are a little above the data at low ω. Full lines show CGA results with CT effects. The FSI have little effect on the cross section at and above the quasi-free peak which is displayed more clearly in Figs. 10–13 drawn with a linear scale.

The deuteron cross section at $\omega \gtrsim \omega_{qf}$ has been used in Refs. [28] and [29] to obtain nucleon form factors and structure functions. Thus, the agreement between theory and experiment for deuteron (e,e') cross sections at $\omega \gtrsim \omega_{qf}$ is not surprising. The CGA and CGA + CT results in Fig. 6 are obtained by the $P(k,E)$ given by Eq. (3.2), whereas the two PWIA results are obtained by the $P(k,E)$ and $P_{RR}(k,E)$ given by Eq. (3.3). The effect of relativistic correction to the energy of the recoiling nucleon is not very significant. In a deuteron the FSI effects are rather small, and the cross section at $\omega<\omega_{qf}$ is primarily determined by the momentum distribution $n_d(k)$. There is a significant increase in the effect of FSI, on the cross section at small ω, in going from ^{2}H to ^{3}He. Thus the cross sections at $\omega \ll \omega_{qf}$ of ^{3}He and heavier nuclei are not primarily determined by their spectral functions. On the linear scale (Fig. 11) it appears that the quasi-free peak is observed in ^{3}He at a slightly higher energy than predicted.

In contrast, the agreement between theory and experiment is not that close in ^{4}He. At low ω the CGA calculation with CT comes closest to data, but it overestimates the cross section. At large ω the FSI effects are negligible, and still the ^{4}He cross section is underestimated by

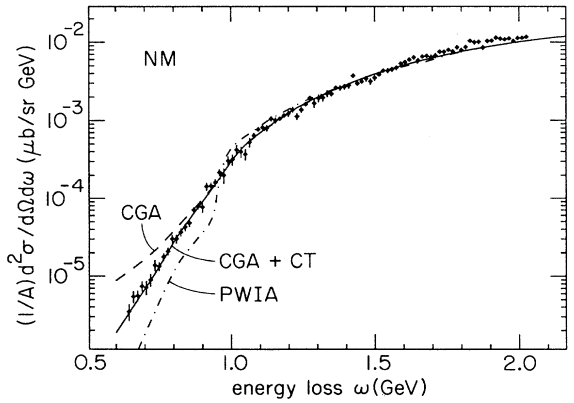

FIG. 9. The experimental and theoretical cross sections for the scattering of 3.595-GeV electrons by 30° from NM (from Ref. [7]). See the caption of Fig. 7 for notation.

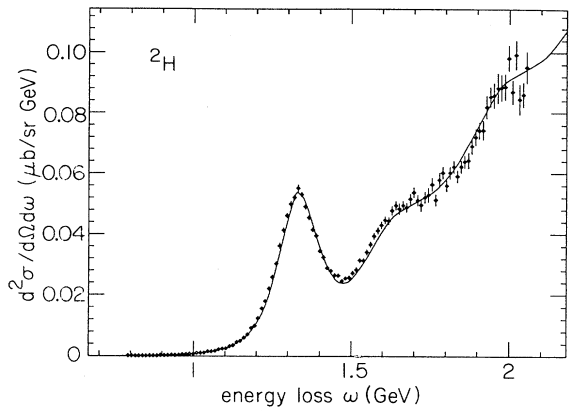

FIG. 10. Figure 6 on a linear scale.

$\sim 10\%$ as can be clearly seen in Fig. 12. We have also calculated the cross section for ^{4}He at $\varepsilon=3.595$ GeV, $\theta=25°$, which corresponds to a $|\mathbf{q}|$ of 1.64 GeV/c at the quasifree peak. The results are compared with the data [4] in Figs. 14 and 15, and the differences between theory and experiment have essentially the same character at this lower value of $|\mathbf{q}|$.

The most likely cause of the disagreement at $\omega \gtrsim \omega_{qf}$ is the neglect of pair currents in the present work. At lower values of $|\mathbf{q}|$ these give a significant contribution to the cross section in the dip region between the quasifree and the Δ peaks [30]. Even in ^{3}He (Fig. 11) a little more cross section in the dip will improve the agreement with the experimental data. The theory also appears to underestimate the NM cross section at $\omega>\omega_{qf}$ as can be seen in Fig. 13. However, it is not clear why the disagreement with the experiment at $\omega>\omega_{qf}$ is much larger in ^{4}He than in ^{3}He and NM.

The folding function $F_q(\omega-\omega')$ takes into account the FSI of a nucleon with the residual system. For this reason, only the PWIA quasielastic cross section is folded with F_q. The products of electron-nucleon inelastic scattering also have FSI, however, these are more difficult to calculate. The inelastic part of the PWIA cross section is rather smooth, and hence it is likely that the FSI

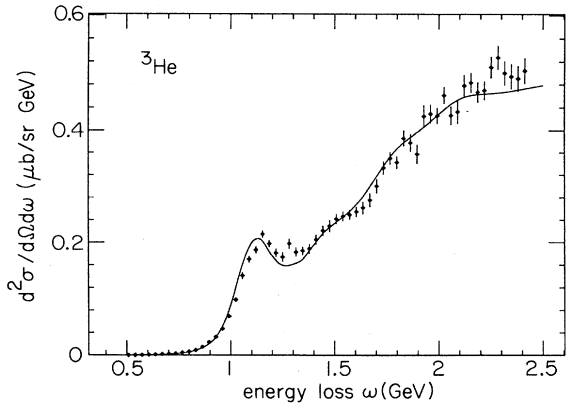

FIG. 11. Figure 7 on a linear scale.

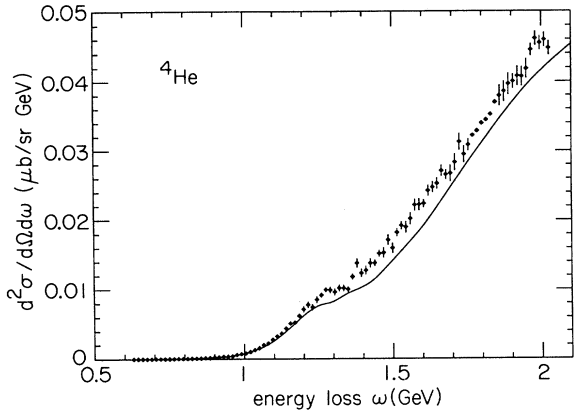

FIG. 12. Figure 8 on a linear scale.

do not have a significant effect on it. Nevertheless, we also calculate the cross section obtained by folding the total PWIA result with F_q. Generally the results of such a calculation are not significantly different from those shown. However, in ^{4}He at $\varepsilon=3.595$ GeV and $\theta=25°$ there is a small perceptible difference at the quasifree peak, between the two calculations as shown in Fig. 15.

The cross sections shown in Figs. 8, 12, 14, and 15 are with the $P_R(k,E)$ calculated with Eq. (3.8). In Fig. 16 we compare the results obtained with $P_R(k,E)$ given by Eqs. (3.7) and (3.8). The PWIA quasielastic cross sections obtained with these two approximations are rather different at small ω particularly because the contribution of $P_R(k,E)$ given by Eq. (3.7) has an artificial threshold. With completely nonrelativistic kinematics it can be easily verified that the PWIA cross sections obtained with approximation (3.7) are zero for $\omega<q^2/4m-E_4$. However, after folding the quasielastic and including the inelastic part, the results obtained with the two $P_R(k,E)$ are rather similar. The artificial structure introduced by the approximation (3.7) is smoothed out by the FSI folding function. Thus the final results do not seem to depend significantly on the treatment of the total momentum of the correlated pair responsible for $P_R(k,E)$.

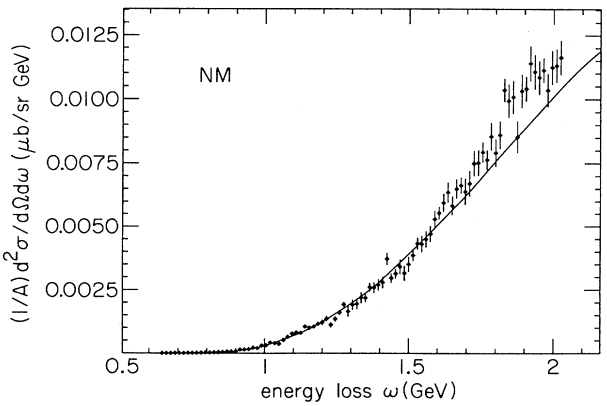

FIG. 13. Figure 9 on a linear scale.

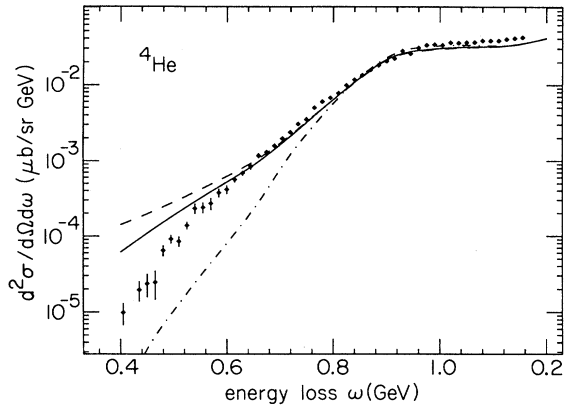

FIG. 14. The experimental and theoretical cross sections for the scattering of 3.595-GeV electrons by 25° from ^{4}He. See the caption of Fig. 6 for notation.

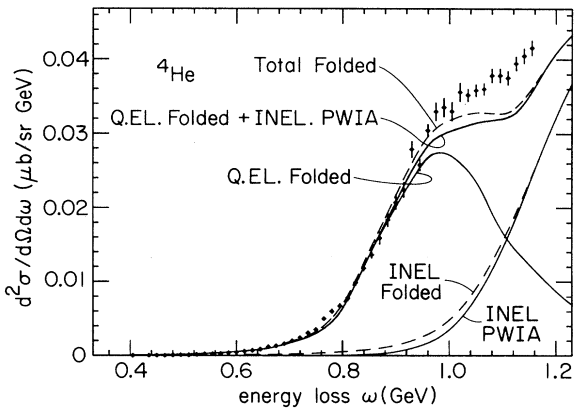

FIG. 15. The experimental and theoretical cross sections for the scattering of 3.595-GeV electrons by 25° from ^{4}He. The full lines show folded quasielastic, PWIA inelastic cross sections, and their sum. The effects of folding the inelastic cross section are shown by dashed lines.

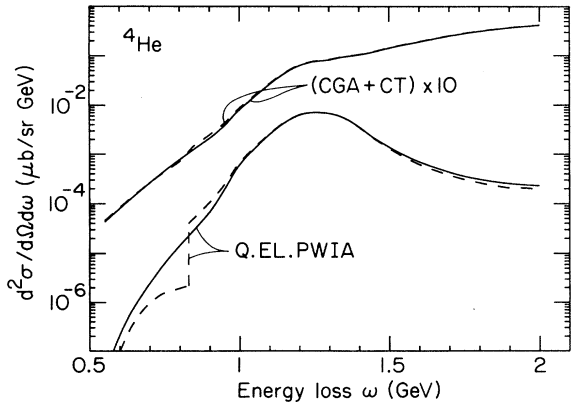

FIG. 16. The quasielastic PWIA and total CGA+CT cross sections for the scattering of 3.595-GeV electrons by 30° from ^{4}He, obtained by Eq. (3.7) and (3.8) are shown by dashed and full lines.

The ^{4}He cross section at small ω comes mostly from FSI in this calculation. Thus, disagreements with experiment at small ω indicate limitations of the CGA folding functions $F_q(\omega-\omega')$. It appears that at $|\mathbf{q}|\sim 2$ GeV/c the calculated cross sections are reasonable at $\omega \gtrsim \omega_{\rm qf}-400$ MeV, suggesting that the CGA $F_q(\omega-\omega')$ is reasonable at $|\omega-\omega'| \lesssim 400$ MeV [Figs. 4(a) and 4(b)]. In ^{2}H and ^{3}He the $F_q(\omega-\omega')$ is very small at $|\omega-\omega'| \gtrsim 400$ MeV, and there is good agreement with data. In NM also there is good agreement with data, however, the ^{4}He $F_q(\omega-\omega')$ appears to be too large at $|\omega-\omega'| \gtrsim 400$ MeV. Note from Fig. 4(b) that in the present calculation the ^{4}He $F_q(\omega-\omega')$ is larger than that for NM at $|\omega-\omega'|>400$ MeV. It could be that the averaging over $\mathbf{r}'_1$, in Eq. (4.14), which is an extra approximation in the calculations for finite nuclei, is partly responsible for the problems in ^{4}He at small ω.

Due to the smallness of the FSI in the deuteron two significant conclusions can be reached from the present studies. The first concerns the use of momentum distribution instead of spectral function in the PWIA. This is equivalent to approximating the $P(k,E)$ in Eq. (2.3) by

$$P(k,E)=n(k)\delta(E-E_R)\ , \tag{5.1}$$

where E_R is an average removal energy. In the deuteron E_R is ~ 0 as indicated by the position of the quasifree peak. The cross section for $\varepsilon=9.76$ GeV, $\theta=10°$, calculated with this approximation, is much too large at small ω (Fig. 17). It thus appears necessary to use the spectral function $P(k,E)$ in the PWIA.

In the deuteron the cross section at small ω is mostly from PWIA while in the larger nuclei, including ^{3}He, it appears that FSI dominate the cross sections at small ω. Thus, only in the deuteron inclusive electron scattering data can be used to study the high-momentum components without significant FSI corrections. The cross sections obtained by artificially setting

$$P(k>1.33\ \text{fm}^{-1},E)=0 \tag{5.2}$$

are shown in Fig. 17. These are significantly below the data, and thus the data confirm the existence of high-momentum components in the deuteron wave function and suggest that $n_d(k)$ predicted with the Argonne model of v_{NN} is reasonable.

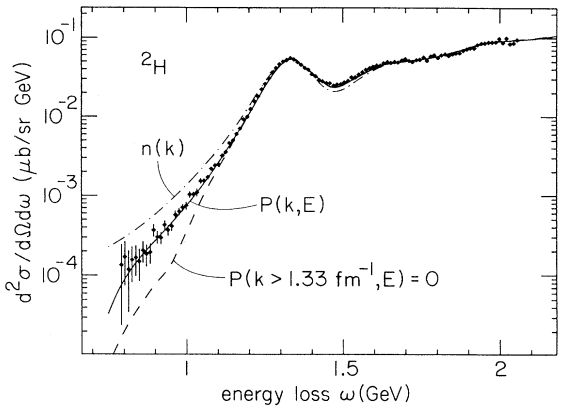

FIG. 17. The experimental and theoretical cross sections for the scattering of 9.76-GeV electrons by 10° from ^{2}H. The full, dashed, and dash-dotted lines show results obtained with the full $P(k,E)$, the $P(k>1.33\ \text{fm}^{-1},E)=0$, and with the $n(k)$.

ACKNOWLEDGMENTS

It is a pleasure to thank Donal Day for providing tables of the data on ^{2}H, ^{3}He, and ^{4}He; Rocco Schiavilla and Robert Wiringa for providing the ^{3}He and ^{4}He Monte Carlo configurations and the momentum distributions of nucleons, deuterons, and tritons in ^{2}H, ^{3}He, and ^{4}He; and Adelchi Fabrocini, Stefano Fantoni, and Ingo Sick for many discussions. This work has been supported by the U.S. National Science Foundation through Grant No. PHY89-21025, and the calculations reported here were made possible by a grant of time on the Cray computers at the National Center for Supercomputing Applications, Urbana, IL.

[1] *Modern Topics in Electron Scattering,* edited by B. Frois and I. Sick (World Scientific, Singapore, 1991).
[2] S. Rock *et al.*, Phys. Rev. Lett. **49**, 1139 (1982).
[3] D. Day *et al.*, Phys. Rev. Lett. **43**, 1143 (1979).
[4] D. Day *et al.*, Phys. Rev. Lett. **59**, 427 (1987).
[5] D. Day *et al.*, Phys. Rev. C **40**, 1011 (1989).
[6] H. Meier-Hajduk, U. Oelfke, and P. U. Sauer, Nucl. Phys. **A499**, 637 (1989).
[7] O. Benhar *et al.*, Phys. Rev. C **44**, 2328 (1991).
[8] W. Czyz and K. Gottfried, Ann. Phys. (N.Y.) **45**, 47 (1963).
[9] I. Sick, D. Day, and J. S. McCarthy, Phys. Rev. Lett. **45**, 871 (1980).
[10] P. Bosted, R. G. Arnold, S. Rock, and Z. Szalata, Phys. Rev. Lett. **49**, 1380 (1982).
[11] R. J. Glauber, in *Lectures in Theoretical Physics,* edited by W. E. Brittin *et al.* (Interscience, New York, 1959).
[12] S. J. Brodsky, in *Proceedings of the XIII International Symposium on Multiparticle Dynamics, Volendam, The Netherlands, 1982,* edited by W. Metzgen, E. W. Kittel, and A. Stergion (World Scientific, Singapore, 1982).
[13] A. Mueller, in *Proceedings of the XVI Rencontres de Moriond, Les Arcs, France, 1982,* edited by J. Tran Thanh Van (Editions Frontières, Gif-sur-Yvette, 1982).
[14] C. Itzykson and J. B. Zuber, *Quantum Field Theory* (McGraw-Hill, New York, 1980).
[15] J. Carlson, V. R. Pandharipande, and R. Schiavilla, in [1].
[16] O. Benhar, A. Fabrocini, and S. Fantoni, in [1].
[17] T. de Forest, Jr., Nucl. Phys. **A392**, 232 (1983).
[18] R. B. Wiringa, R. A. Smith, and T. L. Ainsworth, Phys. Rev. C **29**, 1207 (1984).
[19] C. Ciofi degli Atti, E. Pace, and G. Salmé, Phys. Rev. C **21**, 805 (1980).
[20] H. Meier-Hajduk, Ch Hajduk, P. U. Sauer, and W. Theis, Nucl. Phys. **A395**, 332 (1983).
[21] M. Lacombe, B. Loiseau, S. M. Richard, and R. Vinh

Mau, Phys. Rev. C **21**, 861 (1980).
[22] H. Morita and T. Suzuki, Prog. Theor. Phys. **86**, 671 (1991).
[23] C. Ciofi degli Atti, S. Simula, L. L. Frankfurt, and M. I. Strikman, Phys. Rev. C **44**, 7 (1991).
[24] R. Schiavilla and R. B. Wiringa (private communication).
[25] B. H. Silverman *et al.*, Nucl. Phys. **A499**, 763 (1989).
[26] C. Carraro and S. E. Koonin, Nucl. Phys. **A524**, 201 (1991).
[27] G. L. Farrar, H. Liu, L. L. Frankfurt, and M. I. Strikman, Phys. Rev. Lett. **61**, 1698 (1988).
[28] G. Höhler *et al.*, Nucl. Phys. **B114**, 505 (1976).
[29] A. Bodek and J. L. Ritchie, Phys. Rev. D **23**, 1070 (1981).
[30] J. M. Laget, in [1].